*Mém. Soc. géol. France*, N.S., 1990, n° 156, pp. 85-95
*Mém. Soc. géol. suisse*, 1990, n° 1, pp. 85-95
*Vol. spec. Soc. Geol. Italiana*, 1990, n° 1, pp. 85-95

# The seismic properties of Alpine calcite and quartz mylonites determined from the orientation distribution function

by DAVID MAINPRICE*, MARTIN CASEY** and STEFAN SCHMID**

*Key words*. – Seismic properties, Fabric, Deformation.

*Abstract*. – A straight forward integration method is presented to calculate the elastic and seismic properties of rocks from the even part of the orientation distribution function (ODF). The even part of the ODF has been determined by pole figure inversion using the spherical harmonic method for a series of calcite and quartz mylonites from major Alpine lineaments. Calcite specimens from the Glarus overthrust and Morcles nappe are from the epi-metamorphic zone, corresponding to a upper-crustal environment. The quartz specimens from the Simplon and Insubric lines are from the meso-metamorphic zone, corresponding to a mid-crustal environment. All specimens show extensive signs of plastic deformation and exhibit strong fabrics.

The calculated seismic Vp stereograms correlate well with the major features seen in the crystallographic pole figures. In calcite mylonites the Vp velocity minimum is associated with the c-axes point maximum. The axial nature of the low temperature (300-400°C) calcite fabrics results in large normal incidence reflection coefficients (0.02), hence such mylonites are good reflectors. The Vp values are almost constant within the foliation plane. The quartz fabrics are more complex with a more varied three dimensional character. Vp may vary considerably within the foliation plane whereas the variation between the foliation plane and its normal is less marked. Normal incidence reflection coefficients are typically 0.01, however these values may be increased by compositional changes (eg mica growth).

## Les propriétés sismiques des mylonites alpines à calcite et quartz : calcul par la fonction de distribution des orientations cristallines

*Mots clés*. – Propriétés sismiques, Fabriques, Déformation.

*Résumé*. – Une méthode simple d'intégration est présentée pour calculer les propriétés élastiques et sismiques des roches, à partir des parties paires de la fonction des distributions des orientations cristallines (FDOC). Celle-ci est déterminée par inversion des figures de pôle, utilisant la méthode des harmoniques sphériques, pour une série mylonitique de calcite et de quartz des linéaments majeurs des Alpes. Les spécimens de calcite du chevauchement de Glarus et de la nappe de Morcles proviennent des zones épi-métamorphiques, de croûte supérieure. Les échantillons de quartz de la ligne du Simplon et de la ligne insubrienne proviennent de zones méso-métamorphiques, ce qui correspond à un environnement de croûte moyenne. Tous les spécimens montrent les signes d'une déformation plastique et révèlent de fortes fabriques.

Les stéréogrammes de vitesses sismiques Vp calculées se corrèlent bien avec les observations majeures que l'on peut faire sur les figures de pôles cristallographiques. Dans les mylonites de calcite, la vitesse minimum des ondes P correspond au maximum des axes c. La nature axiale de la fabrique basse température (300-400°C) de la calcite crée, si l'incidence est normale un coefficient de réflexion de 0.02, ces mylonites peuvent être ainsi de bons réflecteurs. Les valeurs de Vp, dans le plan de foliation sont quasi constantes. La fabrique de quartz est plus complexe et a des variations tridimensionnelles. Vp peut varier considérablement à l'intérieur du plan de foliation, néanmoins la variation de Vp entre le plan de foliation et sa normale est moins marquée. Pour une incidence normale, les coefficients de réflexion sont de façon caractéristique 0.01, mais ces valeurs peuvent être augmentées par des changements de composition (par exemple la croissance de mica).

## I. – INTRODUCTION

Over the last 2 years the national Alpine deep continental reflection seismic programs (CROP, ECORS, NFP-20) have revealed a complete two-dimensional picture of several critical sections down to the Moho. In certain seismic sections the lower crust is strongly reflective and relatively homogeneous on a 10 km scale, whereas in other areas strong local reflectors are present, possibly indicative of ductile shear zones or faults. Studies from other continental areas have encountered similar features [for review see Moody and Brocher, 1987]. However the interpretation of such features is not straight forward without a quantitative knowledge of the seismic properties of rocks in the mid to lower crust. In this study we present a means of calculating the complete seismic properties from the orientation distribution fonction (ODF) of monophased mylonites of mid to lower crustal Alpine rocks. The samples studied come from classical Alpine lineaments that may have an expression at depth in the crust (Glarus overthrust, Simplon line, Insubric line).

The origin of the reflective nature of the lower crust has invoked many possible causes. Indeed it is not certain that there is one universal cause of the phenomenon. Among the proposed explanations for the regional horizontal seismic layering are : variation of pore fluid pressure [e.g. Jones and Nur, 1984], fabric variations due to plastic deformation [e.g. Klemperer, 1987], compositional banding [e.g. Hurich and Smithson, 1987], intrusion of igneous sills [e.g. Finlayson *et al.*, 1984]. The localised dipping reflectors are usually attributed to brittle fault or ductile mylonite zones;

* Lab. Tectonophysique, USTL, 34060 Montpellier cedex, France.
** Geologisches Institut, ETH-Zentrum, CH-8092 Zürich, Switzerland.

occasionally the reflector can be correlated with a surface expression of the feature [e.g. Fountain *et al.*, 1984]. In this study we will address the questions : what are the seismic properties of strongly deformed mylonites and are the fabrics of such rocks responsible for the regional reflectivity or localised dipping reflectors. In the discussion, we will indicate what may be the relative importance of other deformation related factors, such as pore fluids or synmetamorphic reactions.

Studies of the type described below also allow us to catalogue the 21 elastic constants of a general triclinic body for each mylonite specimen. Such information is extremely difficult to acquire by traditional techniques such as laboratory measurements under hydrostatic pressure. Such a data basis of elastic constants of real rocks provides ideal data for 3-D seismic modelling. As the national deep seismic programs move to the second phase of operation where the 3-D nature of crust will be a major objective, such 3-D elastic data will be of considerable importance [e.g. Fuchs *et al.*, 1987; Gajewski and Psencik, 1988].

## II. – X-RAY TEXTURE GONIOMETRY

The pole figures were measured at ETH Zurich in the combined reflection and transmission scan method using CoK$\alpha$ radiation. For each specimen eight reflections were measured, for calcite (01.2), (10.4), (11.0), (11.3), (20.2), (01.8), (11.6) and (30.3) and for quartz (10.2), (10.1), (20.1), (10.0), (21.1), (11.0), (11.1) and (11.2). The appropriate corrections were made for defocussing in the reflection mode.

The data were processed using a set of FORTRAN computer programs developed and described by Casey [1981]. The orientation distribution functions (ODF) were calculated from the pole figures using the spherical harmonic method described by Bunge and Wenk [1977] and Bunge [1982]. The convention used for the Eulerian angles ($\psi_1$, $\Phi$, $\psi_2$) of the ODF, which describe the orientation of a crystal with respect to the specimen coordinate frame (e.g. lineation-foliation), are those given by Casey [1981]. The crystal ortho-normal reference frame is chosen such that there is a two-fold axis at Yc with Xc = $\perp$ (10.0) and Zc = $\perp$ (00.1) for both calcite and quartz. The specimen orthonormal reference frame has Xs parallel to the foliation normal and Ys parallel to the lineation. All poles figures are presented with the foliation aligned E-W (verticval) and the lineation horizontal.

## III. – METHOD OF CALCULATION OF SEISMIC PROPERTIES

To calculate the seismic properties from a polycrystal one needs to evaluate the elastic properties of the aggregate. In the case of an aggregate with a fabric the anisotropy of the elastic properties of the single crystal must be taken into account for the calculation of the tensorial properties. For each volume fraction measured at an orientation **g** defined by the three Euler angles ($\psi_1$, $\Phi$, $\psi_2$), the single crystal elastic stiffness matrix $C(\mathbf{g}^o)$ has to be rotated into the specimen coordinate frame using a rotation matrix ($g_{ij}$); viz

$$C(\mathbf{g}) = g_{im}\, g_{jn}\, g_{ko}\, g_{lp}\, C(\mathbf{g}^o)$$

where

$C(\mathbf{g})$ = elastic property in specimen coordinates

$g_{ij} = g\,[\psi_1, \Phi, \psi_2]$ = crystal to specimen coordinates rotation matrix

$\mathbf{g} = [\psi_1, \Phi, \psi_2]$ = measured crystal orientation in sample coordinates

$\mathbf{g}^o = [\psi_1 = 0, \Phi = 0, \psi_2 = 0]$ = crystal reference orientation in sample coordinates.

Using the continuous ODF the elastic properties are averaged over all possible orientations within the asymetric unit defined by the crystal and specimen symmetries. The elastic constants may be calculated by integration over all orientations of the ODF, or calculated from the ODF coefficients of the harmonic method [Wenk *et al.*, 1988]. In the general case of triclinic crystal and specimen symmetry the integration is given by Bunge [1985] as :

$$\bar{C} = \frac{1}{8\Pi^2} \int C(g) \cdot \tilde{f}(g) \sin\Phi \, d\, g$$

where

$\bar{C}$ is the elastic property of the aggregate and

$\tilde{f}(g)$ is the even part of the ODF (where the L index is always even in the series expansion method, [see Bunge, 1982 for details]).

As the elastic properties are 4th order centrosymmetric tensorial properties we have verified by numerical calculation that one needs only expand the even part of the ODF to the fourth order of the L index. The previous statement has four important implications; firstly numerical calculations can be limited to the L $\geq$ 4 of the series expansion with considerable saving of calculation time, secondly the number of pole figures needed to determine the ODF (with L $\geq$ 4) is greatly reduced (only 2 pole figures for trigonal crystal symmetry and triclinic specimen symmetry), thirdly the limitation to L $\geq$ 4 means that only the smooth or "long range" part of the ODF contributes to the elastic properties, and fourthly only the even part of the ODF is required. The even part of the ODF is directly obtained by pole figure inversion in the harmonic method whereas the odd part of the ODF can only be obtained by such techniques using various assumptions [Bunge, 1982].

A Fortran program has been developed by one of us [D.M.] to complement the routines developed by Casey [1981] to undertake the above integration procedure on the expanded ODF. In the case of trigonal minerals the elastic constants are measured in an orthonormal reference frame with Xc = a-axis, Zc = c-axis whereas the ODF uses Xc = m-axis, Zc = c-axis. The difference in reference frame requires a rotation of 90 degrees about the c-axis. An integration step of 10 degrees on each Euler angle provided an acceptable compromise between computation time and accuracy taking into account the "long range" nature of the even ODF with L $\geq$ 4. The angular half-width resolution of such an ODF ($L_{max}$ = 4) can be defined as ($360^o/L_{max}$) = $90^o$, which is much larger than our integration step. The elastic constants are considered to be accurate to two decimal places (in Mb), similar to that of Brillouin scattering for single crystal elastic constants or equivalent to ± 0.05 km/s for minerals considered here.

The final step in the calculation is to evaluate the seismic velocities from the aggregate elastic constants for each direction of interest ($X_i$) over a geographic hemisphere. It is traditional to present this as the solution of the Christoffel equation [e.g. Crosson and Lin, 1971; Peselnick *et al.*, 1974] defined as

$$\det | T_{ik} - \delta_{ik} \rho V^2 | = O$$

where $\delta_{ik}$ is the Kronecker's delta, $\rho$ is the density, V is one of the three seismic velocities and $T_{ik}$ the Christoffel stiffnesses.

The procedures developed here are capable of calculating the Voigt, Reuss or Voigt-Reuss-Hill (V-R-H) elastic averages. The Voigt average assumes a homogeneous elastic deformation throughout the polycrystal, whereas the Reuss average assumes a homogeneous stress throughout. Neither is physically realistic and Hill [1952] suggested taking the mean of the two values (V-R-H) which has no physical justification but often produces values close to the measured ones. Measurements on the Twin Sisters dunite by Crosson and Lin [1971] have shown that seismic P-wave velocities calculated using the Voigt average give the closest agreement between petrofabric derived and laboratory measured seismic velocities. A similar study on an anorthosite by Seront *et al.* [1989] also showed the Voigt average to be in closest agreement, hence we have elected to use Voigt average in all calculations.

## IV. – GEOLOGICAL SETTING-MICROSTRUCTURES AND FABRICS OF SPECIMENS

The specimens come from two distincts Alpine metamorphic terrains (fig. 1) defined by Frey *et al.* [1980]. The calcite mylonites come from the middle and southern part of the Helvetic nappes and lie within the epi-metamorphic zone of Tertiary Alpine age. Typical metamorphic temperatures and pressures in this zone are 300-400°C and 200-300 MPa, corresponding to 8-10 km depth or an upper crustal continental tectonic environment.

The quartz mylonite samples from the Simplon and Insubric lines formed under lower greenschist to lower amphibolite facies conditions with typical temperatures and pressures of 400-600°C and 400-600 MPa, corresponding to 12-20 km depth. These quartz mylonites occur in a mid to uppercrustal environment and along two Alpine fault zones with a strong vertical component of movement, postdating Lepontine Tertiary amphibolite grade metamorphism in the Pennine nappes. The same two lineaments, observed at the surface, extended to greater depth where their traces are expected to cross the NFP-20 West (Simplon) and NFP-20 South (Insubric line) seismic transects at mid- to lower crustal levels (other contributions, this volume).

### 1) Calcite mylonites

Three calcite mylonites from the study of Schmid *et al.* [1981] have been studied here. Samples 7816 and 71 are from the inverted limb of the Morcles nappes, SW Switzerland (fig. 1). Sample 7816 has a particularly strong fabric

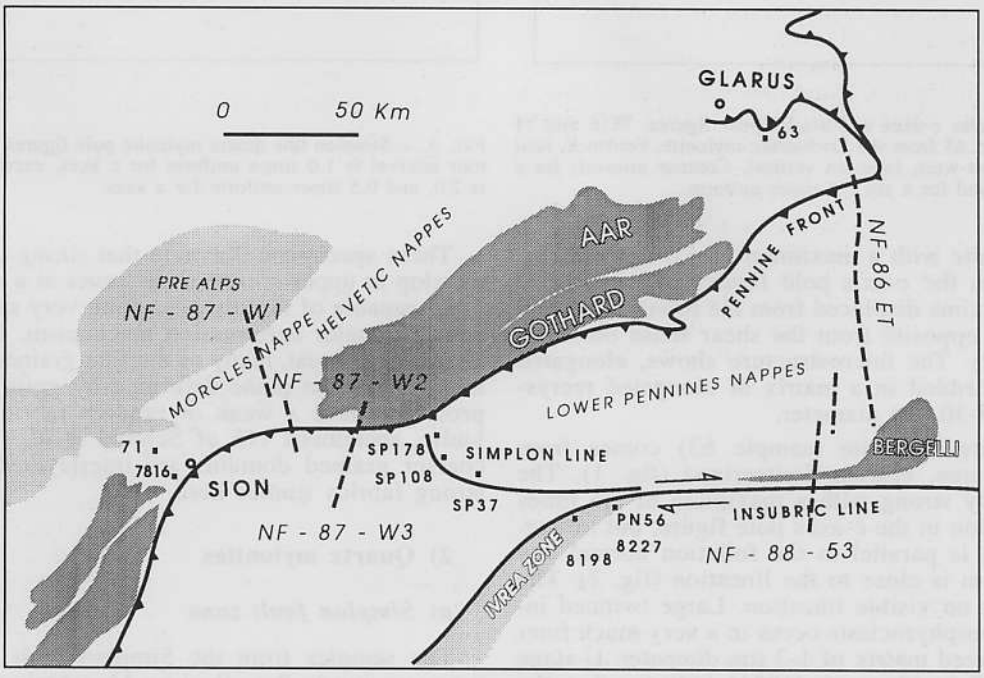


FIG. 1. – Simplified geological map of the Swiss Alps. The calcite mylonite localities in the Morcles nappe (71, 7816) and Glarus overthrust (63). The Simplon line (SP 178, SP 108, SP 37) and Insubric line (PN 56, 8227, 8198) quartzite mylonite localities.

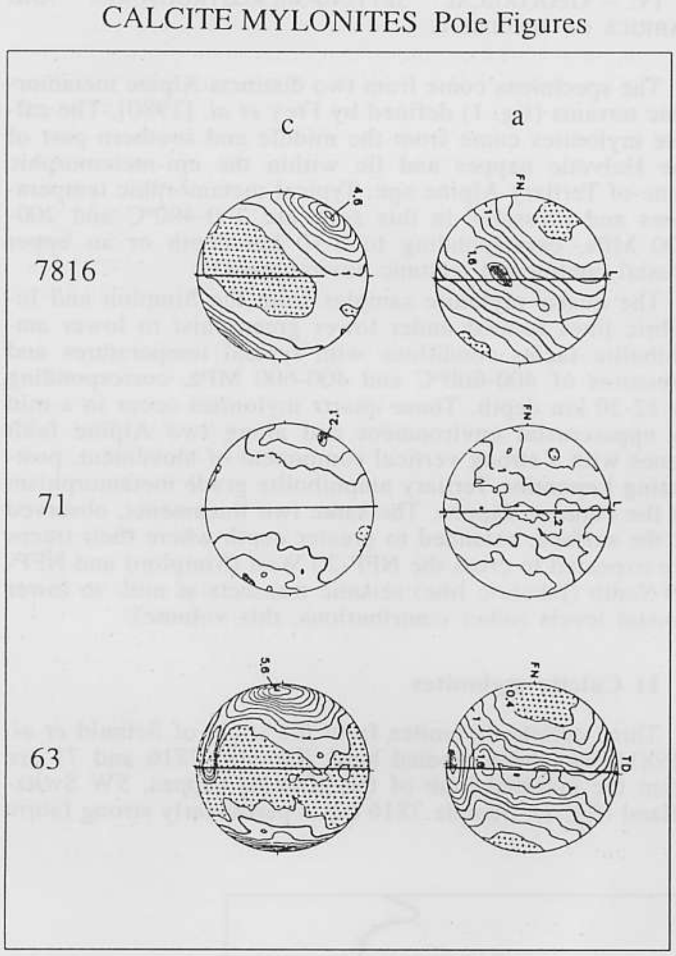


FIG. 2. – Calcite mylonite c-axes and a-axes pole figures. 7816 and 71 from the Morcles nappe. 63 from the Lochseiten mylonite, Foostock, near Glarus. Lineation in east-west, foliation vertical. Contour intervals for c are 0.5 times uniform and for a are 0.2 times uniform.

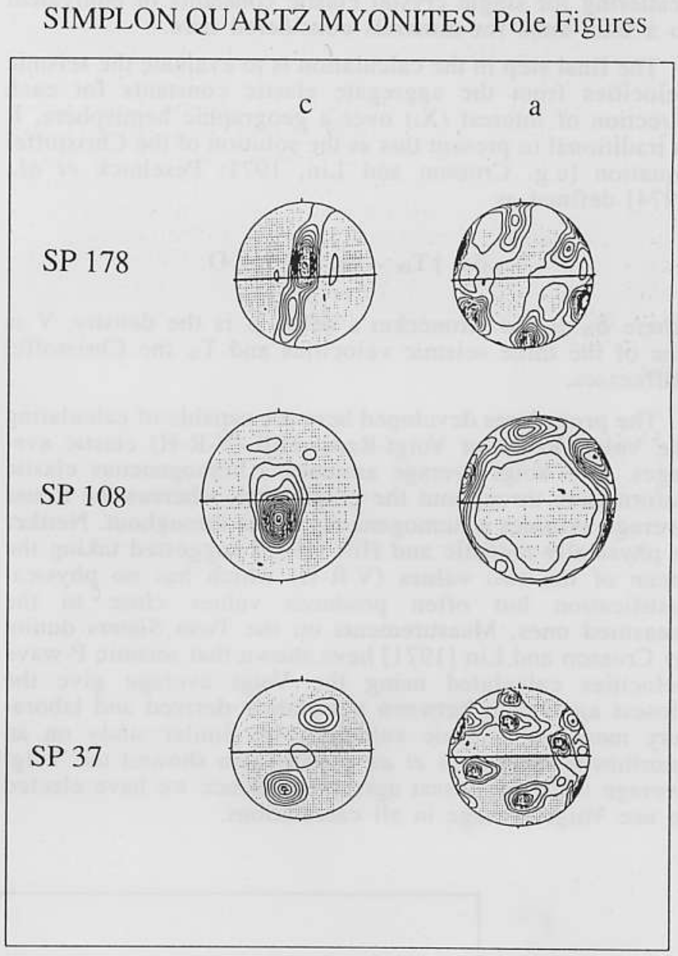


FIG. 3. – Simplon line quartz mylonite pole figures for c and a axes. Contour interval is 1.0 times uniform for c axes, except for SP 37 where it is 2.0, and 0.5 times uniform for a axes.

for a calcite mylonite with a maximum of 4.6 times a uniform distribution in the c-axis pole figure. In both specimens the c-axis maxima displaced from the foliation normal by 40°, in a sense opposite from the shear sense observed in the field (fig. 2). The microstructure shows, elongated porphyroclasts embedded in a matrix of elongated recrystallized grains of 5-30 µm diameter.

The other calcite mylonite (sample 63) comes from Glarus overthrust area, eastern Switzerland (fig. 1). The fabric is particularly strong with a maximum of 5.6 times a uniform distribution in the c-axes pole figure, but in contrast the maximum is parallel to the foliation normal and the a-axes maximum is close to the lineation (fig. 2). The hand specimen has no visible lineation. Large twinned intensively strained porphyroclasts occur in a very much finer equiaxed recrystallized matrix of 1-3 µm diameter. U-stage measurements by Schmid *et al.* [1981] indicate that the strong fabric is essentially due to the strongly aligned prophyroclasts in a nearly random matrix.

These specimens illustrate that strong calcite fabrics can develop in upper crustal shear zones at a depth where twinning, capable of rapidly producing very strong textures, becomes a major deformation mechanism. In the case of the Glarus overthrust, many of the fine-grained mylonites found along the thrust plane deformed by grain boundary sliding processes have a weak or random fabric (Lochseiten mylonite, specimens 115 of Schmid *et al.* [1981]). However, coarser grained domains are interlayered and exhibit the strong fabrics studies here.

### 2) Quartz mylonites

#### *a) Simplon fault zone*

The samples from the Simplon fault zone (SFZ) have been previously described by Mancktelow [1987a, 1987b]. The samples were collected from strongly deformed quartz veins between the Simplon pass and San Lorenzo (fig. 1).

Deformation occurred in greenschist to lower amphibolite facies conditions with a relative downthrow of 12 km of the SW block [Mancktelow, 1985] in a normal fault geometry. Fabrics found along the SFZ show single c-axes girdles (e.g. SP 178) inclined with respect to foliation (fig. 3). Often the girdles are dominated by a strong single concentration (e.g. SP 178) or several isolated concentrations (e.g. SP 37). Some samples have "atypical textures" [Mancktelow, 1987b] with a strong c-axis maximum at the center of pole figure and a tendency for orientation of the a-axes to be weakly constrained in a plane normal to the c-axis maximum (e.g. SP 108). The microstructure is elongated ribbon grains with recrystallised grains of about 80 µm diameter. SP 108 has grain growth producing an oblique shape fabric.

### *b) Insubric line*

The three specimens come from the Insubric mylonite belt accompanying the Insubric line (fig. 1). This mylonite belt accommodates vertical (steep backthrust) and horizontal components (dextral) of movement [Schmid *et al.*, 1987].

INSUBRIC QUARTZ MYLONITES Pole Figures

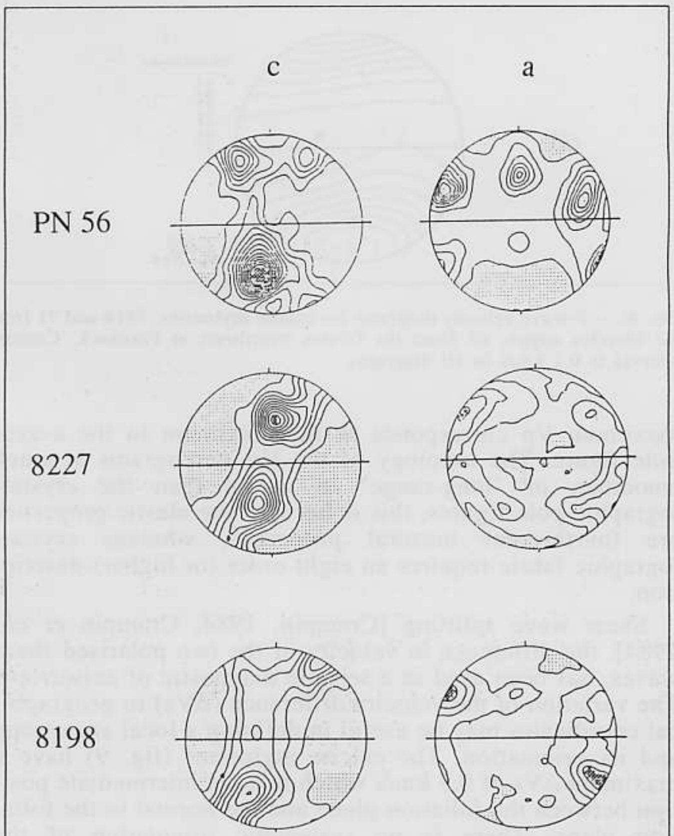


FIG. 4. – Insubric line quartz mylonite pole figures for c and a axes. Contour interval is 0.5 times uniform for all pole figures.

Specimen PN56 is a quartzo-feldspathic mylonite derived from a pegmatitic dyke within meta-diorites of the Ivrea zone. These Ivrea lithologies have been mylonitized under greenschist facies conditions and now form the southern part of the Insubric mylonite belt 1.5 km SW of Arcegno. The microstructure is composed of extremely elongated quartz porphyroclasts (20 : 1 axial ratio) with recrystallized grains of about 10 µm diameter. The c-axis fabric has a poorly developed cross-girdle which is almost perpendicular to the lineation with a strong concentration in one hemisphere (fig. 4).

Specimen 8227 is a mylonitic quartz vein collected within granitic mylonites 1 km SE of Arcegno. These mylonites are derived from the Sesia tectonic unit and they form the northern part of the Insubric mylonite belt. The microstructure is dominated by the development of the oblique shape preferred orientation of the quartz grains, sutured grain boundaries and very fine recrystallized grains. The c-axes pole figure shows a well developed asymmetric girdle with two strong maximas (fig. 4). Specimen 8198 is again a quartz vein within granitic mylonites, 1 km N of Scaredi in Val Loana, near the northern boundary of the Insubric line mylonites. The microstructure exhibits elongate (2 : 1 axial ratio) recrystallized quartz grains of about 50 µm diameter, slightly oblique to the foliation. The c-axis pole figure has a up-right cross girdle with a strong asymmetric maximum (fig. 4). Both specimens from the granitic Insubric mylonites (8227, 8198) indicate a dextral shear sense, whereas the fabric asymmetry of specimen (PN 56) is much less pronounced in the case of the c-axis pole figure, but marked in the case of the a-axis pole figure.

## V. – SEISMIC PROPERTIES

Before considering the seismic properties calculated from the ODF of the polycrystals it is useful to recall those of the single crystals. The P-wave velocities of calcite and quartz single crystals in figure 5 were calculated using the elastic constants given by Dandekar [1968] and McSkimin *et al.* [1965], respectively. Both minerals are trigonal and hence there is a three fold symmetry of the property with respect to the c-axis. However the velocity distributions are quite different, the maximum Vp being close to m-axis in calcite, whereas it is near the normal to the rhombohedral plane in quartz. Both minerals have significant P-wave anisotropy coefficients [$A = (V_{max} - V_{min}) / V_{max}$]; calcite A = 27.7 % and quartz A = 24.3 %.

The calcite mylonite P-wave velocities vary between 7.1 and 6.2 km/s (fig. 6). The fast directions are essentially contained in the foliation with a minimum normal to the foliation; the symmetry is axial. The anisotropy coefficients vary between 5.7 % and 12.0 %. The velocity only varies by 0.1 km/s in the foliation (horizontal) plane in specimens 71 and 63 illustrating that the velocity is isotropic in this plane.

The quartzite mylonite P-wave velocities from the Simplon line vary between 5.7 and 6.6 km/s (fig. 7). The minimum velocity is parallel to the lineation in all three specimens. The maximum velocity is contained in an in-

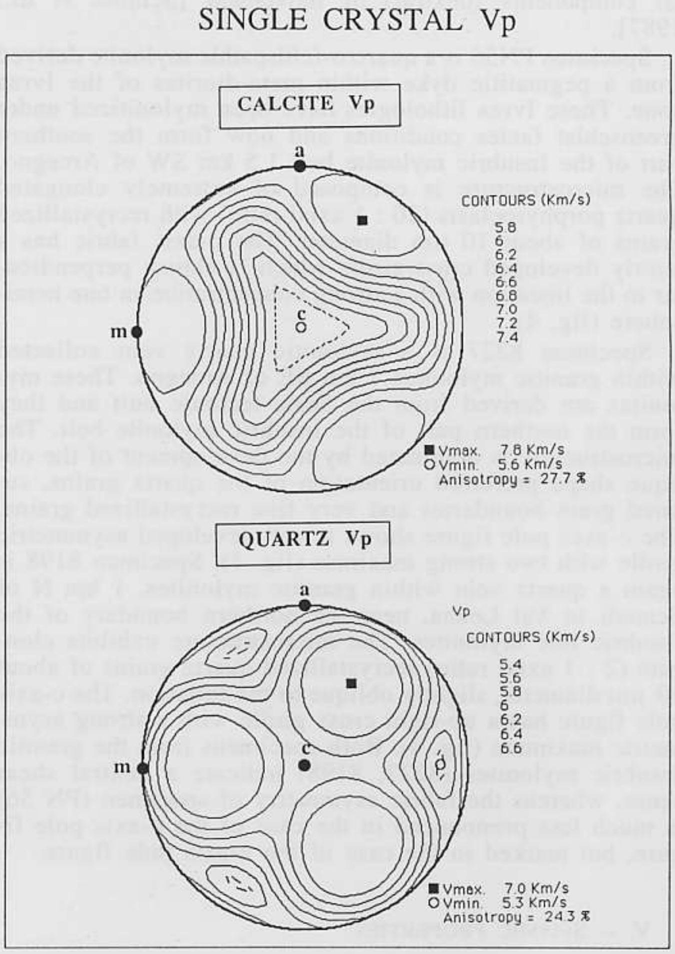


FIG. 5. – P-wave velocity diagrams for calcite and quartz single crystals. Calculated using the elastic constants given by Dandekar [1968] for calcite and McSkimin *et al.* [1965] for quartz. Contour interval 0.2 km/s.

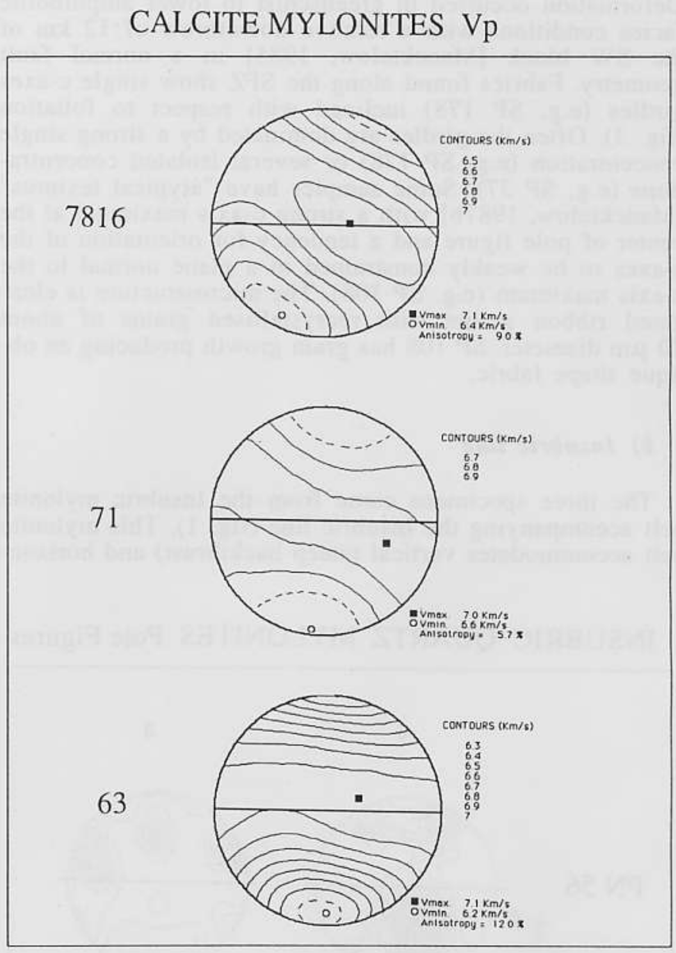


FIG. 6. – P-wave velocity diagrams for calcite mylonites. 7816 and 71 from the Morcles nappe, 63 from the Glarus overthrust at Foostock. Contour interval is 0.1 km/s in all diagrams.

clined girdle, roughly normal to the lineation in all cases. The velocity distributions are somewhat more complicated than those of the calcite mylonites, in particular there is a greater variation in velocity in the foliation plane (0.6 km/s) than between the foliation plane and its normal (~ 0.5 km/s). The property is truly triclinic in symmetry, A is around 11 % for all three specimens.

The quartzite mylonites from the Insubric line have P-wave velocities that vary between 5.8 km/s and 6.7 km/s (fig. 8). Specimen PN 56 shows a particulary striking P-wave variation with A = 14.2 %. Both the maximum and the minimum are close to the foliation plane with a 0.6 km/s variation in the foliation. In contrast, specimens 8227 and 8198 have a weaker anisotropy (A = 7.8 % and 6.9 %) with the minimum parallel to the lineation, the maximum in an inclined girdle about the minimum.

In all these Vp diagrams a clear relationship can be seen between the crystallographic and velocity fabric. In calcite the maximum Vp corresponds to the maximum in the a-axes pole figure and the minimum Vp corresponds to the maximum in the c-axes pole figure. Similarly in quartz the maximum Vp corresponds to the maximum in the a-axes pole figure. The topology of the Vp stereograms is much smoother, or "long-range" in nature than the crystallographic pole figures, this is because the elastic properties are fourth-order tensoral properties, whereas crystallographic fabric requires an eight order (or higher) description.

Shear wave splitting [Crampin, 1984; Crampin *et al.*, 1984], the difference in velocity of the two polarised shear waves, has been used as a seismic diagnostic of anisotropy. The variation of the velocity difference ($\Delta$Vs) in geographical coordinates may be useful in defining a local anisotropy and its orientation. The calcite mylonites (fig. 9) have a maximum $\Delta$Vs of 0.3 km/s which is in an intermediate position between the foliation plane and the normal to the foliation plane. There is no systematic orientation of the minimum $\Delta$Vs. The Simplon quartzites and PN56 from the Insubric line have a maximum $\Delta$Vs of between 0.6 and 0.8 km/s, which are extremely high values. The maximum and minimum $\Delta$Vs values have a complex distribution and no systematic pattern is observed (figs. 10, 11).

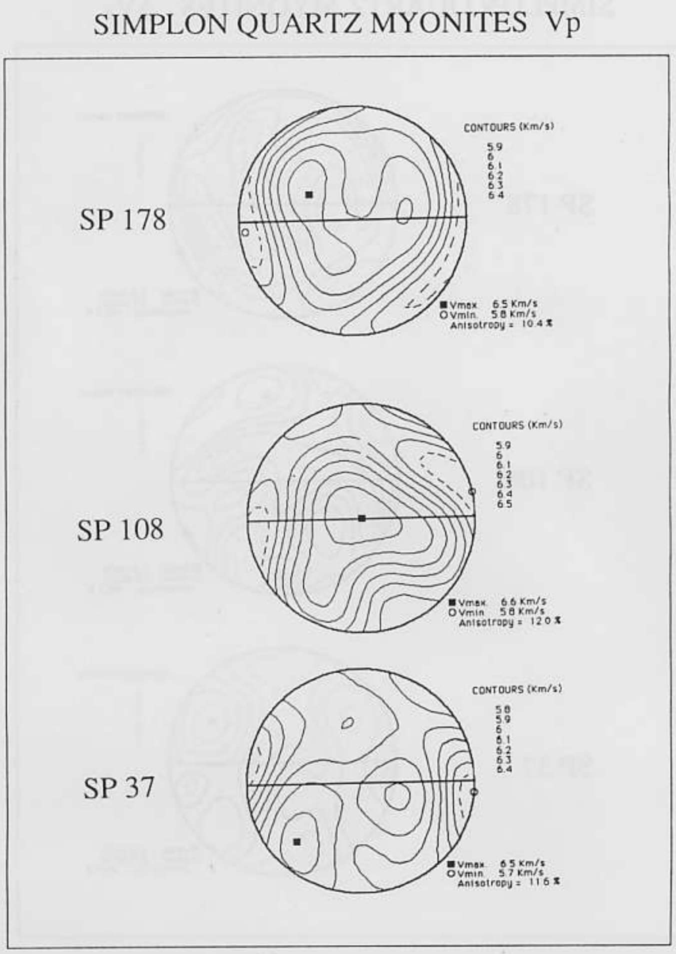


FIG. 7. – P-wave velocity diagrams for the Simplon line quartz mylonites. Contour interval is 0.1 km/s in all diagrams.

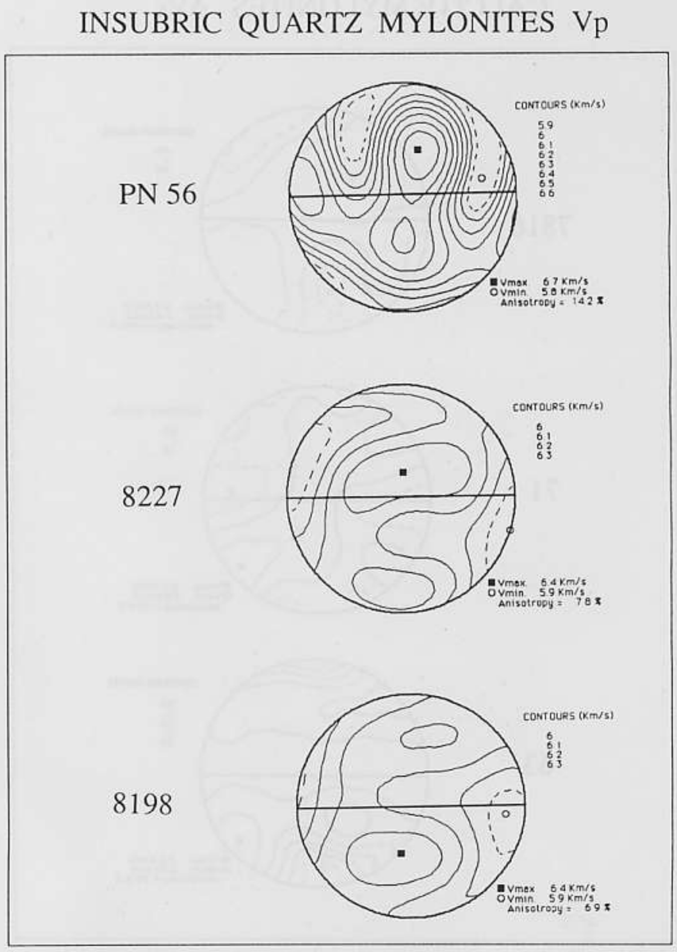


FIG. 8. – P-wave velocity diagrams for the Insubric line quartz mylonites. Contour interval is 0.1 km/s.

## VI. – DISCUSSION

The calculated Vp values indicate there is a direct relationship between the seismic velocity stereograms and the crystallographic pole figures. In calcite the Vp minimum corresponds to the maximum in the c-axes pole figure and in quartz there is a strong similarity between the Vp minimum and the a-axis (or m-axis) pole figure. If we assume the foliation is horizontal, the epi-metamorphic (LT) calcite fabrics give rise to a strong vertical Vp anisotropy, whereas the meso-metamorphic quartz fabrics give rise to a strong horizontal Vp anisotropy. Hence seismic reflections may be produced by the LT calcite fabrics. A strong three dimensional anisotropy is produced by quartz fabrics which is characterized by a strong c-axis point maximum (e.g. SP 108; figs. 3 and 7). Such fabrics will result in vertical and horizontal Vp anisotropy producing reflections and azimuth variations.

The Vp anisotropies calculated for these samples are quite strong, 5.7 to 14.2 % when compared to mantle peridotites with typical values of 8-9 %. The continental crustal environment is mineralogically more heterogeneous than the mantle and the attitude of the foliation more variable (as shown by large scale folding), hence the seismic reflectivity or azimuth variation will depend to some extent on the properties of the rocks surrounding these crustal mylonites. The Voigt average $V_p$ values for a randomly orientated calcite and quartz polycrystalline aggregates are 6.83 and 6.19 km/s, respectively. Hence, for normal incidence, the reflection coefficient ($R_c$), (i.e. the ratio of the amplitude of the reflected wave to that of the incident wave) is given by

$$R_c = (\rho^m Vp^m - \rho^r Vp^r)/(\rho^m Vp^m + \rho^r Vp^r)$$

where ρ is the density, super scripts m and r signify mylonite and random fabric rocks, respectively. As a first model we can assume that the monophased mylonites develop within in a calcite or quartz layer, hence $\rho^m = \rho^r$ and the reflection coefficient is uniquely defined by the change in velocity between the non-deformed random fabric rocks and the mylonite rocks. In some cases, for example at Glarus [Schmid *et al.*, 1981], we may have a random

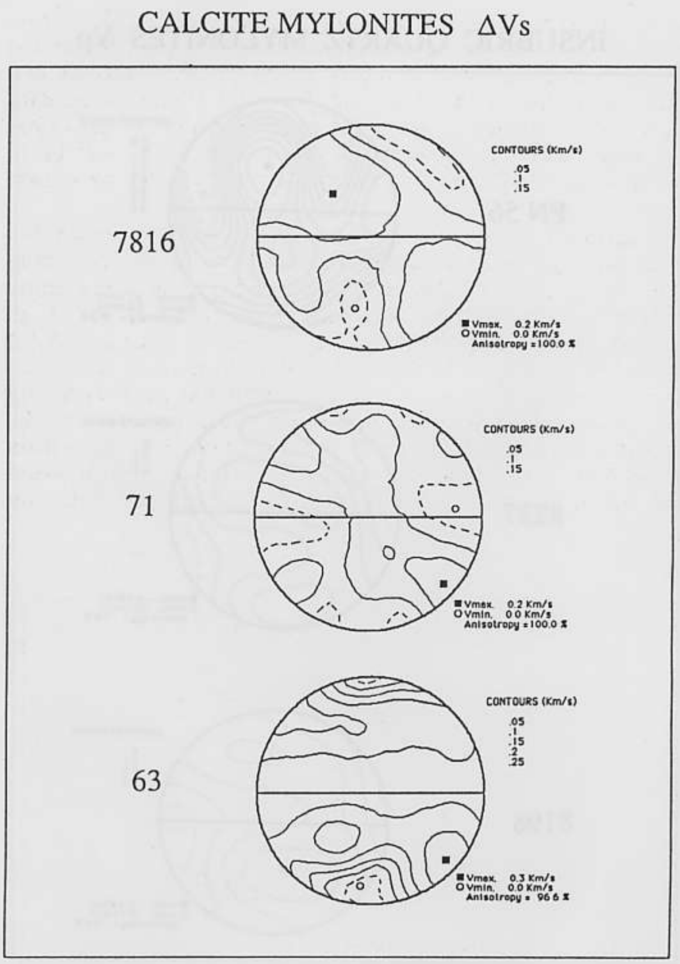


FIG. 9. – Shear wave splitting (ΔVS) diagrams for the calcite mylonites.

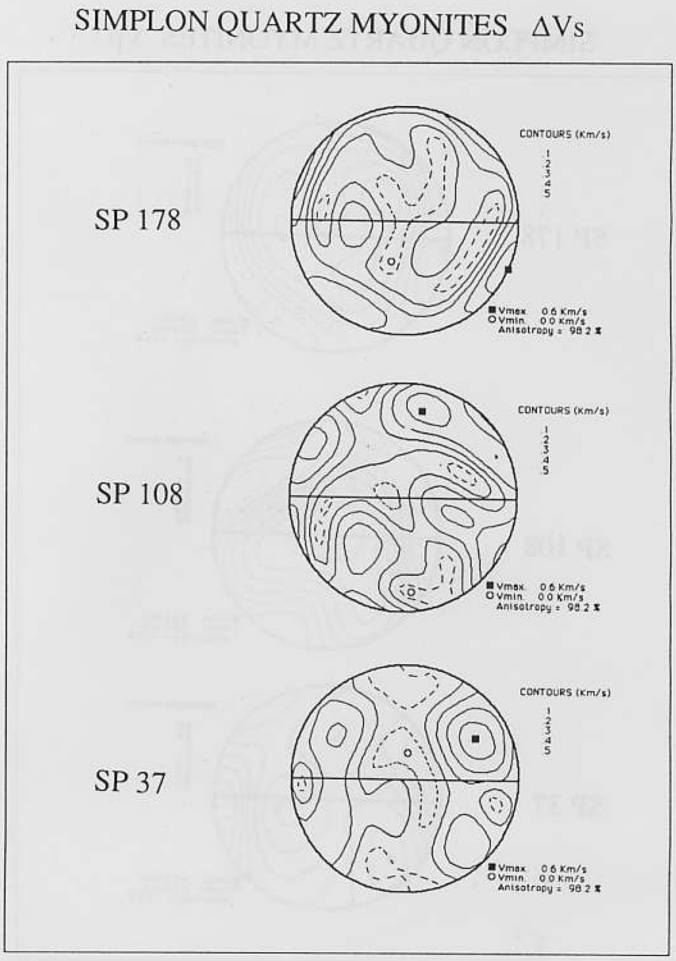


FIG. 10. – Shear wave splitting (ΔVS) diagrams for the Simplon line quartz mylonites.

fabric mylonite in the most intensely deformed zone surrounded by mylonites with strong fabrics. In such situations a random/non-random sequence may be repeated several times. For normal incidence the calcite mylonites produce reflections coefficients of 0.02 whereas the quartz mylonites have coefficients of 0.01 or less, indicating the stronger reflectivity of the calcite mylonites. Strong seismic reflections can be expected for Rc values greater than 0.01, [see examples in McDonough and Fountain, 1988]. Hence in the dominantly limestone composition Helvetic nappes, the presence of mylonite zones should give relatively strong seismic reflections, whereas the quartzite mylonite zones give weaker reflections.

The lower crust is mineralogically complex and the development of shear zones (mylonites) often engenders the development of mineralogical as well as textural changes. The mineralogical changes have two effects on the seismic properties : firstly the bulk density of the aggregate changes and, secondly the new mineral may have a strong fabric (for example mica). The most extreme case is certainly the growth of mica in retrograde shear zones; mica has a density of 2.911 g/cm$^3$ (cf. calcite 2.717 g/cm$^3$, quartz 2.65 g/cm$^3$) and has a strong Vp anisotropy, A = 44.1 %. Hence the addition of 20 % mica to a rock, for example will strongly effect the seismic properties. The P-wave velocity contribution of mica fabrics to seismic properties can be easily evaluated using c-axis pole figures as Vp is essentially axial about this direction (fig. 12). Mica c-axes pole figures typically have strong point maxima normal to foliation [e.g. Lipshie *et al.*, 1976] which produce a Vp minimum normal to the foliation (fig. 12). To illustrate the effect of mica we have added 20 % mica to 80 % quartz (SP 108, figs. 3 and 7). The result is in fact a lowering of the Vp anisotropy from 12.0 % to 10.5 %, however the anisotropy normal to the foliation has increased. The increase of the foliation normal anisotropy with increasing mica content will produce an increase in the normal incidence reflection coefficient, hence the quartz mylonite will become a stronger seismic reflector. The mica effect will be particularly important in retrograde quartz-feldspar mylonites where feldspar breaks down to give mica [Kern and Wenk, 1989].

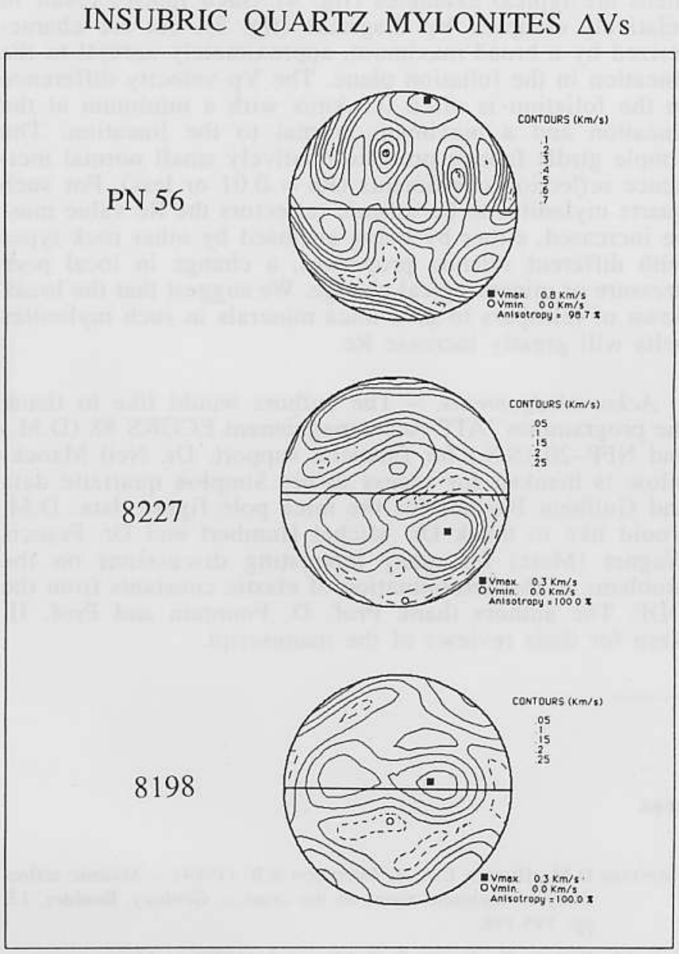


FIG. 11. – Shear wave splitting (ΔVS) diagrams for the Insubric line quartz mylonites.

Pore fluid pressure is another effect often cited in connection with the reflectivity of mylonite zones [e.g. Jones and Nur, 1984] or the reduction of seismic velocities [Hyndman and Klemperer, 1989]. Fluid pressure has three effects, reduction of density ($\rho$) as the fluid is essentially water with $\rho = 1.0$ g/cm$^3$, a change in the bulk elastic properties and crack or fluid distribution anisotropy. The density effect can be important as most silicates that occur in the lower crust have a density of between 2.0 and 3.0 kg/cm$^3$, (e.g. quartz $\rho = 2.65$ g/cm$^3$, plagioclase $\rho = 2.68$ g/cm$^3$). The reduction of density will result in an increase of seismic velocity as $Vs \propto 1/\sqrt{\rho}$, however this is overshadowed by the change in the elastic stiffnesses ($C_{ij}$). The bulk elastic properties decrease in value with increasing fluid pressure, the exact manner in which they vary will depend on the fluid distribution or microstructure. For example, fluid pressure may be distributed homogeneously on 120° triple boundaries resulting in a homogeneous change in elastic properties. In another case fluid may be localised in a fracture array resulting in anisotropic elastic and seismic properties [Garbin and Knopoff, 1975; Hudson, 1982]. In mylonite zones the grains are often elongated parallel to the lineation and flattened in the foliation plane. Fractures can open up either parallel to the foliation plane, a general plane of weakness, or normal to the lineation in tensional pull-apart fractures. The effect of fluid pressure will be to lower seismic velocities and may alter the anisotropy in mylonite zones.

Depending on the magnitude of deviatoric stresses the local pore pressure in mylonites will result in fracturing either parallel to $\sigma_1$ (low $\sigma_1 - \sigma_2$ values) or at some angle (typically 30°) to $\sigma_1$ up to a maximum value of 45° (high $\sigma_1 - \sigma_2$ values). Given that the mylonites fabrics exhibit asymmetries indicating non-coaxial deformation it is reasonable to suggest that $\sigma_1$ will be inclined at approximately 45° to the foliation. Assuming such stress orientation, the fractures resulting from local pore pressure will be within 30° or less of the foliation orientation. Hence pore pressure will increase the anisotropy associated with the foliation plane.

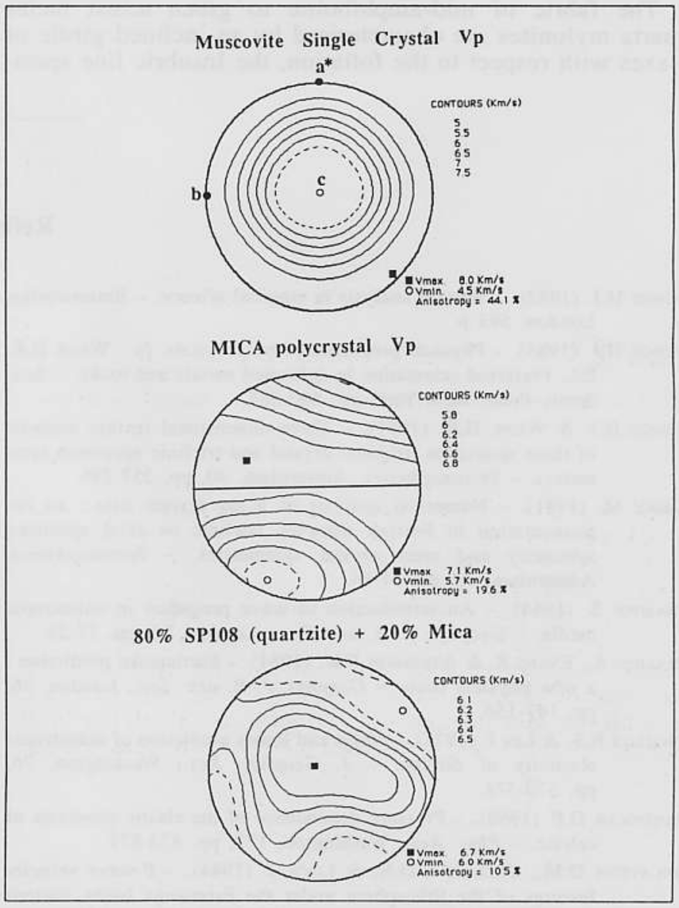


FIG. 12. – P-wave velocity diagrams for the muscovite single crystal, mica polycrystal and quartzite SP 108 with 20 % mica. The single crystal diagram was calculated using the elastic constants given by Vaughan and Guggenheim [1986]. The mica polycrystal diagram was calculated using the c-axis polefigure measured from an Ivrea zone gneiss measured by G. Barruol.

## VII. – Conclusions

Mylonite zones with strong fabrics can produce strong seismic reflectors when the fabric type is simple, as in the case of low temperature calcite mylonites. Other topologically simple fabrics are present in some quartz mylonites (e.g. SP 108 fig. 3) where a point maximum may lie parallel to the lineation or normal to the lineation within the foliation plane [see examples in Schmid *et al.*, 1981; Schmid and Casey, 1986; Mainprice *et al.*, 1986]. Such fabrics are characteristic of the highest temperature deformation regime, often just above or below the α-β quartz transition [Mainprice *et al.*, 1986]. PT conditions of the α-β quartz transition correspond approximately to the amphibolite-granulite facies boundary, and the variation of seismic properties across the transition has been studied by Kern [1979]. So we suggest that except for conditions at or below the lower amphibolite facies, the quartz mylonites will produce seismic properties typical of these specimens presented here. These fabrics are expected to be widespread within quartz mylonites in middle to lower crustal extension zones of major tectonic lines such as the Insubric line.

The fabric of mid-amphibolite to green schist facies quartz mylonites are characterised by an inclined girdle of c-axes with respect to the foliation, the Insubric line specimens are typical examples (fig. 4). Such fabrics result in relatively complex Vp diagrams (fig. 8), but are characterized by a broad maximum, approximately normal to the lineation in the foliation plane. The Vp velocity difference in the foliation is often 0.5 km/s with a minimum at the lineation and a maximum normal to the lineation. The simple girdle fabrics produce relatively small normal incidence reflection coefficients (Rc = 0.01 or less). For such quartz mylonites to be seismic reflectors the Rc value must be increased, either by being enclosed by other rock types with different seismic properties, a change in local pore pressure or mineralogical change. We suggest that the break down of feldspars to give mica minerals in such mylonites belts will greatly increase Rc.

*Acknowledgements.* – The authors would like to thank the programmes 'ATP Accompagnement ECORS 88 (D.M.) and NFP–20 (S.S.) for financial support. Dr. Neil Mancktelow is thanked for access to his Simplon quartzite data and Guilhem Barruol for the mica pole figure data. D.M. would like to thank Dr. Michel Humbert and Dr. Francis Wagner (Metz) for many interesting discussions on the problems of the determination of elastic constants from the ODF. The authors thank Prof. D. Fountain and Prof. H. Kern for their reviews of the manuscript.

## References

Bunge H.J. (1982). – Texture analysis in material science. – Butterworths, London, 593 p.

Bunge H.J. (1985). – Physical properties of polycrystals. *In* : Wenk H.R. Ed., Preferred orientation in deformed metals and rocks. – Academic Press, New York, pp. 507-525.

Bunge H.J. & Wenk H.R. (1977). – Three-dimensional texture analysis of three quartzites (trigonal crystal and triclinic specimen symmetry). – *Tectonophysics*, Amsterdam, 40, pp. 257-285.

Casey M. (1981). – Numerical analysis of X-ray texture data : an implementation in Fortran allowing triclinic or axial specimen symmetry and most crystal symmetries. – *Tectonophysics*, Amsterdam, 78, pp. 51-64.

Crampin S. (1984). – An introduction to wave progation in anisotropic media. – *Geophys. J. R. astr. Soc.*, London, 76, pp. 17-28.

Crampin S., Evans R. & Atkinson B.K. (1984). – Earthquake prediction : a new physical basis. – *Geophys. J. R. astr. Soc.*, London, 76, pp. 147-156.

Crosson R.S. & Lin J. (1971). – Voigt and Reuss prediction of anisotropic elasticity of olivine. – *J. Geophys. Res.*, Washington, 76, pp. 570-578.

Dandekar D.P. (1968). – Pressure dependence of the elastic constants of calcite. – *Phys. Rev.*, Washington, 172, pp. 873-877.

Finlayson D.M., Collins C.D.N. & Lock J. (1984). – P-wave velocity features of the lithosphere under the Eromanga basin, eastern Australia including a prominent Mid-Crustal (Conrad ?) discontinuity. – *Tectonophysics*, Amsterdam, 101, pp. 267-291.

Fountain D.M. (1976). – The Ivrea-Verbano and Strona-Ceneri zones, northern Italy : a cross-section of the continental crust-new evidence from seismic velocities of rock samples. – *Tectonophysics*, Amsterdam, 33, pp. 145-165.

Fountain D.M., Hurich C.A. & Smithson S.B. (1984). – Seismic reflectivity of mylonite zones in the crust. – *Geology*, Boulder, 12, pp. 195-198.

Frey M., Bucher K., Frank E. & Mullis J. (1980). – Alpine metamorphism along the geotraverse Basel-Chiasso, a review. – *Eclogae Geol. Helv.*, Basel, 73/2, pp. 527-546.

Fuchs K., Bonjer K.P., Gajewski D., Lueschen E., Prodehl C., Sandmeir K.J., Wenzel F. & Wilhelm H. (1987). – Crustal evolution of the Rhinegraben area. I. Exploring the lower crust in the Rhinegraben rift by unified geophysical experiments. *In* : Z. Ben-Avraham Ed., Sedimentary basins within the Dead Sea and other rift zones. – *Tectonophysics*, Amsterdam, 141, pp. 261-275.

Gajewski D. & Psencik I. (1988). – Ray synthetic seismograms for a 3-D anisotropic lithospheric structure. – *Phys. Earth. Planet. Int.*, Amsterdam, 51, pp. 1-23.

Garbin H.D. & Knopoff L. (1975). – Elastic moduli of a medium with liquid-filled cracks. – *Q. Appl. Math.*, London, 33, pp. 301-303.

Hill R. (1952). – The elastic behaviour of a crystalline aggregate. – *Proc. Phys. Soc.*, London, A65, pp. 349-354.

Hudson J.A. (1982). – Overall properties of a cracked solid. – *Math. Proc. Cam. Phil. Soc.*, Cambridge, 88, 371-384.

Hurich C.A. & Smithson S.B. (1987). – Compositional variation and the origin of deep crustal reflections. – *Earth Planet. Sci. Lett.*, Amsterdam, 85, pp. 416-426.

Hyndman R.D. & Klemperer S.L. (1989). – Lower crustal porosity from electrical measurements and inferences about composition from seismic velocities. – *Geophys. Res. Lett.*, Washington, 16, pp. 255-258.

JONES T.D. & NUR A. (1984). – The nature of seismic reflections from deep crustal shear zones. – *J. Geophys. Res.*, Amsterdam, 89, pp. 3153-3171.

KERN H. (1979). – Effect of high-low quartz transition on compressional and shear wave velocities in rocks under high pressure. – *Phys. Chem. Mineral.*, Berlin, 4, pp. 161-171.

KERN H. & WENK H.-R. (1989). – Fabric-related velocity anisotropy and shear-wave splitting in rocks from the Santa Rosa mylonite zone, California. – *J. Geophys. Res.*, Washington, (in press).

KLEMPERER S.L. (1987). – Reflectivity of the crystalline crust : hypotheses and tests. – *Geophys. J.R. astr. Soc.*, London, 89, pp. 217-222.

LIPSHIE S.R., OERTEL G. & CHRISTIE J.M. (1976). – Measurement of preferred orientation of phylosilicates in schists. – *Tectonophysics*, Amsterdam, 34, pp. 91-99.

MAINPRICE D., BOUCHEZ J.L., BLUMENFELD P. & TUBIA J.M. (1986). – Dominant C-slip in naturally deformed quartz : implications for dramatic plastic softening at high temperature. – *Geology*, Boulder, 14, pp. 812-822.

MANCKTELOW N.S. (1985). – The Simplon line : a major displacement zone in the western Lepontine Alps. – *Eclogae Geol. Helv.*, Basel, 78, pp. 73-96.

MANCKTELOW N.S. (1987a). – Quartz textures from the Simplon fault zone, southwest Switzerland and north Italy. – *Tectonophysics*, Amsterdam, 135, pp. 133-153.

MANCKTELOW N.S. (1987b). – A typical textures in quartz veins from the Simplon faults zone. – *J. Struct. Geol.*, Oxford, 9, pp. 995-1005.

McDOUNOUGH D.T. & FOUNTAIN D.M. (1988). – Reflection characteristics of a mylonite zone based on compressional wave velocities of rock samples. – *Geophys. J.*, New York, 93, pp. 547-558.

McSKIMIN H.J., ANREATCH J.R. & THURSTON R.N. (1965). – Elastic moduli of quartz versus hydrostatic pressure at 25° and – 195.8°C. – *J. Appl. Phys.*, Washington, 36, pp. 1624-1632.

MOODY W.D. & BROCHER T.M. (1987). – Coincident seismic reflection/refraction studies of the continental lithosphere : a global review. – *Rev. Geophys.*, Washington, 25, pp. 723-742.

NICOLAS A. & CHRISTENSEN N.I. (1987). – Formation of anisotropy in upper mantle peridotites – a review. – *Rev. Geophys.*, Washington, 25, pp. 111-123.

PESELNICK L., NICOLAS A. & SETEVENSON P.R. (1974). – Velocity anisotropy in a mantle peridotite from the Ivrea zone : application to the upper mantle anisotropy. – *J. Geophys. Res.*, Washington, 79, pp. 1175-1182.

SCHMID S.M., CASEY M. & STARKEY J. (1981). – An illustration of the advantage of a complete texture analysis described by the orientation distribution function (ODF) using quartz pole figures data. – *Tectonophysics*, Amsterdam, 78, pp. 101-117.

SCHMID S.M., CASEY M. & STARKEY J. (1981). – The microfabric of calcite tectonites from the Helvetic nappes (Swiss Alps). *In :* "Trusts and nappe tectonics". – *Geol. Soc.*, London, pp. 151-158.

SCHMID S.M. & CASEY M. (1986). – Complete fabric analysis of some commonly observed quartz c-axis patterns. – *AGU monograph*, Washington, 36, pp. 263-286.

SCHMID S.M., ZINGG A. & HANDY M. (1987). – The kinematics of the movements along the Insubric line and the emplacement of the Ivrea zone. – *Tectonophysics*, Amsterdam, 135, pp. 47-66.

SERONT B., MAINPRICE D. & CHRISTENSEN N.I. (1989). – The complete seismic properties of an anorthosite-comparison between LPO and laboratory measurements. – *EOS*, Washington, 70, pp. 460-461.

VAUGHAN M.T. & GUGGENHEIM S. (1986). – Elasticity of muscovite and its relationship to crystal structure. – *J. Geophys. Res.*, Amsterdam, 91, pp. 4657-4664.

WENK H.R., JOHNSON G.C. & MATTIES S. (1988). – Direct determination of physical properties from continuous orientation distributions. – *J. Appl. Phys.*, Washington, 63, pp. 2876-2879.